LA-UR-81-1835

TITLE: GLOBAL KINETICS FOR THE SHOCK-INDUCED DECOMPOSITION OF HETEROGENEOUS EXPLOSIVES

AUTHOR(S): JERRY WACKERLE AND ALLAN B. ANDERSON

MASTER

SUBMITTED TO: THE SYMPOSIUM ON KINETICS OF CHEMICAL AND PHYSICAL PROCESSES, FOR THE PROCEEDINGS OF THE TENTH NORTH AMERICAN THERMAL ANALYSIS SOCIETY CONFERENCE.

University of California

LOS ALAMOS SCIENTIFIC LABORATORY
Post Office Box 1663 Los Alamos, New Mexico 87545
An Affirmative Action/Equal Opportunity Employer

Form No. 836 R3
St. No. 2629
12/78

UNITED STATES
DEPARTMENT OF ENERGY
CONTRACT W-7405-ENG-36

GLOBAL KINETICS FOR THE SHOCK-INDUCED DECOMPOSITION OF HETEROGENEOUS EXPLOSIVES*

Jerry Wackerle and Allan B. Anderson
Los Alamos National Laboratory
University of California
Los Alamos, NM 87545

ABSTRACT

We have developed methods to determine empirical rate laws for the shock-induced decomposition of condensed explosives. Pressure-field histories are measured with embedded gauges in plane-wave shock-initiation experiments. A Lagrangian analysis is used to integrate the fluid-dynamic conservation relations, giving the histories of density and energy fields in the reactive flow. A reactant-product equation of state is assumed and a global reaction progress variable, λ, and the associated reaction rate, $\dot{\lambda}$, are calculated. Correlations of the rate to other state variables provide empirical rate laws, which prove successful in the numerical modeling of numerous initiation and detonation phenomena.

For heterogeneous explosives, we obtain excellent correlations and modeling with the form:

$$\dot{\lambda} = Z_o \, p_s^n (1-\lambda) \, e^{-T^*/T} \quad ,$$

where p_s is the shock pressure, T is the current temperature, and Z_o, n and T* are constants. Heterogeneous explosive rate laws combining three factors--shock-strength, depletion, and heating--are consistent with many shock-initiation observations and the favored "nucleation and growth" concept of shock-induced decomposition. The strong correlation to a simple Arrhenius heating factor is remarkable, because the temperature is an average, equilibrium quantity calculated from the equation of state, yet the formation of local high-temperature regions, or hotspots, is the dominant reaction mechanism in heterogeneous explosives. We discuss possible physical implications of the Arrhenius correlation, and other choices for the three rate factors.

GLOBAL KINETICS FOR THE SHOCK-INDUCED DECOMPOSITION OF HETEROGENEOUS EXPLOSIVES

Jerry Wackerle and Allan B. Anderson
Los Alamos National Laboratory
University of California
Los Alamos, NM 87545

INTRODUCTION

The shock-induced decomposition associated with the initiation and detonation of condensed explosives is a challenging study connecting reactive fluid dynamics and chemical kinetics. Such investigations deal with pressures up to 50 GPa (1 GPa = 10^4 bars), temperatures from 350 to 3500 K, and specific energy release in the kJ/g realm occurring at 0.1- to 100-μs^{-1} rates. Even if good submicrosecond-resolution temperature measurements could be made in this environment,[1] the other state variables vary so much that a purely thermal determination of the decomposition kinetics is impractical. Consequently, we use dynamic, in-material pressure measurements,* the fluid-dynamic conservation relations, and a limited knowledge of the explosive equation of state to derive empirical rate laws for the global decomposition kinetics.

The rate laws are obtained by the following procedure:

(1) Planar shock initiation experiments with embedded pressure gauges are used to determine the pressure histories at a number of Lagrangian positions (that is, at mass points that move with the flow) in the initiating explosive.

(2) A Lagrange analysis is done to obtain, by interpolation, the pressure-field histories, and to integrate the conservation relations for the velocity-, density-, and energy-field histories throughout the distance-time region of the observations.

(3) A global reaction progress variable is defined and incorporated into a pressure-density-energy equation of state, and the decomposition rate calculated throughout the reactive flow.

(4) Position-independent correlations of the rate with the other thermodynamic variables are sought, and when found, formulated as empirical rate laws for the decomposition kinetics.

(5) These rate laws are tested for general validity with numerical hydrodynamic simulation of shock-initiation experiments that are quite different from those generating the rates.

In addition to our work, Soviet investigators have reported the successful use of the above procedure, through step (4), for cast trinitrotoluene (TNT).[3,4] Extensive assessments of alternative experiments, analyses and state equations, but no determinations of decomposition rates, have been reported by other American investigators.[5-8] Our work has included the calculation of rates

---

*As discussed in Ref. 2, in-material velocity gauging or combinations of velocity and pressure measurements can be used for this purpose; for brevity, the use of velocity gauges will not be dis-

for pressed pentaerythritol tetranitrate (PETN),[9] PBX 9404*[10] and 1.8-g/cm^3 (7% porous) pressed triaminotrinotrobenzene (TATB).[11] In both of the latter investigations, we found an excellent rate correlation with the "Direct Analysis Generated Modified Arrhenius Rate" (DAGMAR) form. As well as having a temperature dependence that is almost universal to chemical kinetics, this empirical rate has a strong relation to shock strength.

In the following sections, we will outline the various steps in our procedure for deriving decomposition kinetics, using the results on TATB as an example. In a final section we discuss the implications of DAGMAR, and some more physical alternatives.

EXPERIMENT

The gas-gun experiments are designed to introduce a planar shock wave into an explosive specimen, and to provide one-dimensional reactive flow behind the shock during the time of the embedded-gauge measurements. The arrangement used for TATB is shown in Fig. 1. Target assemblies are fabricated by embedding a low-resistance, four-terminal, Manganin gauge in a grooved disk of TATB, and cementing a flat cover disk of the explosive over it. The gauges are photoetched from 40-μm thick annealed foil and are bonded between two 0.25-mm thick sheets of FEP Teflon. Approximately 60-A currents for the 20-mΩ gauges are provided by two power supplies of the type described by Vantine and coworkers.[12] Their calibration data are used to calculate pressures from the measured resistance change.[13] Electrical pin contactors provide timing fiducials and a measurement of projectile velocity.

Repeated experiments with a 1.17-mm/μs (±0.02 mm/μs) projectile velocity gave an average input shock strength of 7.6 GPa. In 1.8-g/cm^3 TATB, a sustained shock of this amplitude builds up to a 30-GPa detonation wave in about 9 mm of run in slightly less than 2 μs. Gauge data obtained at six locations, ranging from the impact face to a depth of 7.7 mm into the target, are shown as solid lines in Fig. 2.

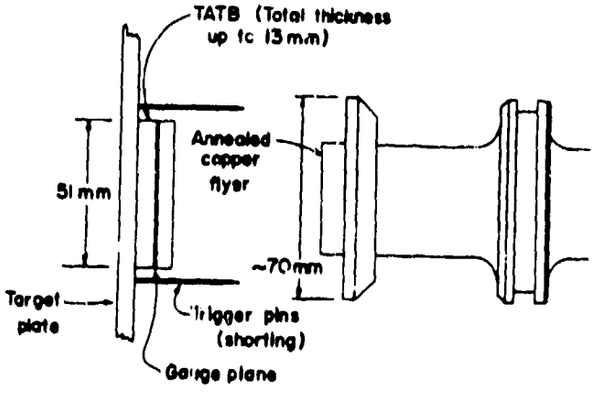

Fig. 1. Target and projectile for sustained-shock gas-gun experiments.

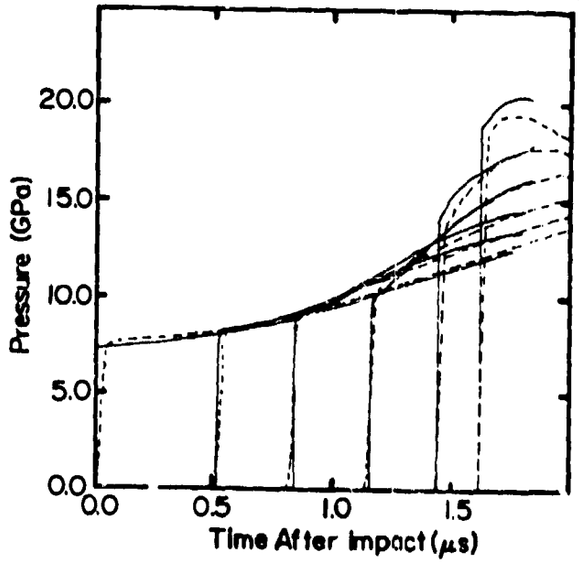

Fig. 2. Observed and calculated pressure histories.

*A plastic bonded HMX, 0.94 cyclotrimethylene trinitramine/ 0.03 nitrocellulose/0.03 tris (β-chloroethyl)-phosphate.

LAGRANGE ANALYSIS

The analysis of gauge data is effected by the successive integration of the fluid-dynamic conservation relations for momentum, mass and energy. In terms of the initial Lagrangian position coordinate, h, and time, t, these relations are:

$$\partial u/\partial t = - v_o \, \partial p/\partial h \quad , \qquad \partial v/\partial t = v_o \, \partial u/\partial h \quad ,$$

and $$\partial e/\partial t = -p \, \partial v/\partial t = -p \, v_o \, \partial u/\partial h \quad .$$

where p, u, v, and e are the pressure, particle velocity, specific volume and specific internal energy, respectively, and the sub-o denotes the initial, unshocked, value. In our treatments of the PETN and PBX 9404 data, we used a "direct analysis" method to numerically integrate the above equations. An incremented, h-t mesh was constructed over the data space, and the analysis was conducted by stepping ahead in small time steps. Simple finite-difference algorithms were used between space increments to calculate gradients and to sum the time increments for the integrations. For each time step, the calculation was performed over the entire space between the impact face and shock front, adding data to the calculation as the front passed a gauge and dropping data as records terminated. While this method gave useful results, it suffered from the need for artificial smoothing and less-than-optimal use of data.

For our TATB study, we adopted a "pathline method" similar to that developed by Seaman.[14] For this, we transform from a real time coordinate to a defined pathline, t(h) and use directional derivatives to replace the gradients $\partial p/\partial h$ and $\partial u/\partial h$. In integral form, the transformed equations become

$$u(h,t) = u_1(h) - v_o \int_{t_1(h)}^{t(h)} \left[\frac{dp}{dh} - \frac{\partial p(h,t')}{\partial t'} \frac{dt'(h)}{dh} \right] dt' \quad ,$$

$$v(h,t) = v_1(h) + v_o \int_{t_1(h)}^{t(h)} \left[\frac{du}{dh} - \frac{\partial u(h,t')}{\partial t'} \frac{dt'(h)}{dh} \right] dt' \quad ,$$

$$e(h,t) = e_1(h) - v_o \int_{t_1(h)}^{t(h)} p(h,t') \left[\frac{du}{dh} - \frac{\partial u(h,t')}{dt'} \frac{dt'(h)}{dh} \right] dt' \quad .$$

Here the total derivatives are along the pathline and the partial derivatives are at fixed t or h, and the sub-1 indicates values along the first path. While the transformation might be suspected of introducing greater error in the analysis, this is not the case. No error is produced by dt/dh, because we choose t(h) arbitrarily, and $\partial p/\partial t$ is evaluated through dense data (unlike $\partial p/\partial h$). In addition, paths can be chosen to minimize the change in pressure, so that the evaluation of dp/dh is generally superior to that of $\partial p/\partial h$.

In our use of the pathline method, we choose the shock locus as the first path, and construct the other paths so that all the gauge data are used throughout the calculation (see Fig. 3). State parameters along the shock path are defined by the Hugoniot relations for conservation of momentum, mass and energy:

$v_o p_1 = u_1 U_1$, $v_1/v_o = 1 - (u_1/U_1)$, and $e_1 - e_o = (p_1/2)(v_o - v_1)$

where U_1 is the shock velocity. We complete this description by specifying the shock Hugoniot for the explosive in the common form $U_1 = C + Su_1$, with the constants C and S evaluated from auxiliary (usually explosive wedge) experiments. The interpolation schemes, sequence of integrations, and numerical algorithms for stepping ahead between pathlines are similar to those used in the direct analysis.

With either method, the fitting of real (estimated to be accurate within 5%) data is somewhat of an exercise in curve fitting. The calculated specific volumes and energies essentially depend on the curvature of p(h), whether taken at constant time or along a pathline. We have found that fitting p(h) with mathematical splines (that minimize the total curvature) gives good results relatively free of unphysical oscillations in v and e. Results are also improved with the imposition of fluid-dynamic and consistency constraints on the fitting, as detailed in Refs. 10 and 11.

EQUATION OF STATE AND RATE CALCULATION

The Lagrange analysis provides a history of pressure, specific volume and energy at the gauge locations, and relating a reaction progress variable to these three state variables allows the calculation of global decomposition rates throughout. The rates are, of course, valid only for the particular equation-of-state relationship chosen.

Equations of state are commonly formulated assuming that the decomposing explosive is a mixture of unreacted solid and fully reacted (mostly) gas products. The relationship is thus a construct of the p-v-e equations for the two components, a reaction progress variable equal to the mass fraction of one of the components (we use that of the products, denoting λ=0 as unreacted and λ=1 as fully reacted), and a "mix rule" that, explicitly or implicitly, divides the specific internal energy between the two components.

Presently, we use the HOM equation of state.[15] The component state relationships are both Mie-Grüneisen forms, that is:

$$p(v,e) = p_r(v) + (\Gamma/v)\ (e-e_r)$$

where $\Gamma = v(\partial p/\partial e)$ is the Grüneisen ratio and the sub-r denotes values along a reference curve. For the solid, this reference is taken as the shock Hugoniot, calibrated to measurements as described above, and the good approximation of (Γ/v) = constant is assumed. The reference curve for the products is taken as the insentrope through the Chapman-Jouget (CJ) detonation state expressed in the Becker-Kistiakowsky-Wilson form.[15] While this is a calculated relationship, it is well calibrated to shock-wave data on product species and to detonation velocities of the well-studied explosives. The mix rule is defined with the assumptions of ideal mixing of the specific volume and energy and of equilibrium of pressure and temperature between the two components. Temperatures along reference curves for the two components are defined by the equation-of-state assumptions already stated, and are calculated at points off these reference curves with the additional assumption of constant specific heat.

The reference curves for 1.8-g/cm^3 TATB are shown in Fig. 4. While the Hugoniot is an accurate (to experimental error) representation of the unreacted states behind the shock, the CJ isentrope indicates only the vicinity of the projection of the fully reacted p-v-e surface. Projections of the partial-reaction surfaces are more-or-less evenly spaced between the Hugoniot and

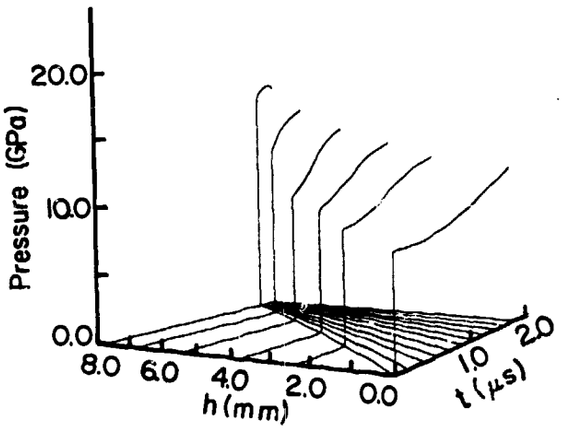

Fig. 3. Pressure histories and sample pathlines.

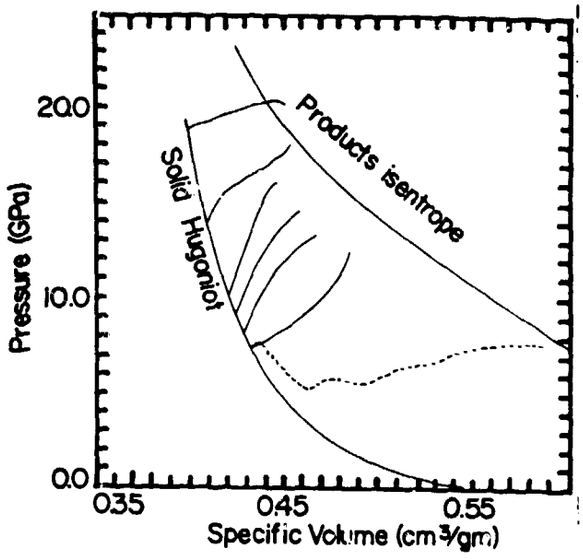

Fig. 4. State paths at gauge locations.

The pressure-specific volume paths derived from the Lagrange analysis of the TATB data are indicated in Fig. 4 as the solid lines originating on the Hugoniot. With the HOM equation of state, the solution for the reaction coordinate, $\lambda(p,v,e)$, is a double-iterative process, which we performed with an algorithm and computer program developed by Forest.[16] Numerical time differentiation of λ provides the calculations of the rate histories, $\dot{\lambda}$, at the different gauge locations, shown as solid lines in Fig. 5. Comparison of Fig. 5 with Fig. 2 shows that relatively modest rates are attained near the impact face, but that substantially higher rates develop as the shock strength increases and the process approaches the transition to a steady detonation. In our subject explosive, 30- to 40-μs^{-1} peak decomposition rates are attained in a detonation wave.

RATE CORRELATION

The analysis at this point provides numerical values of the pressure, density, internal energy, temperature, degree of decomposition and reaction rate at each gauge location. If correlations of the rate values to combinations of other state variables can be found that hold throughout the reactive flow, they can serve as empirical rate laws for the explosive. The calculated "data" can also serve to test various proposed theoretical or empirical rate forms.

With both PBX 9404 and TATB, we have obtained the best results by examining the rate dependence on temperature in a simple Arrhenius form. Assuming first-order depletion, the calculated rates for TATB are shown by the solid curves in Fig. 6. The results are similar to those obtained with PBX 9404, and suggest the same form for the rate. The parallel curves suggest the use of a single activation energy or temperature for the rate, but some modification of the pre-exponential factor is necessary. Because both this factor and the shock strength are monotonically increasing for the deeper gauge locations, it seems appropriate to introduce some measure of shock strength into the rate. Using the shock pressure, p_s, as this measure, we examined the correlation

$$\dot{\lambda} = \quad n \quad -T^*/T$$

calculated rates. A least squares analysis, minimizing deviations in the "experimental" rate-time space of Fig. 5, gives the set of constants: Z_o = 0.0158, n = 2.61 and T* = 1861 K, where μs^{-1} rates and GPa pressure units are used. The correlation to the calculated rates with these constants is indicated by the dashed lines in Figs. 5 and 6.

The correlation is essentially the same as that first obtained with PBX 9404, where analysis of both sustained- and short-shock initiation configurations with a 2.9-GPa input shock strength (but run distance to detonation similar to the TATB experiments) gave Z_o = 0.17, n = 2 and T* = 1200 K as constants.[10] The DAGMAR form for PBX 9404 also included a modest induction time factor, but this may have resulted from a constraint imposed on the direct analysis performed for that explosive.

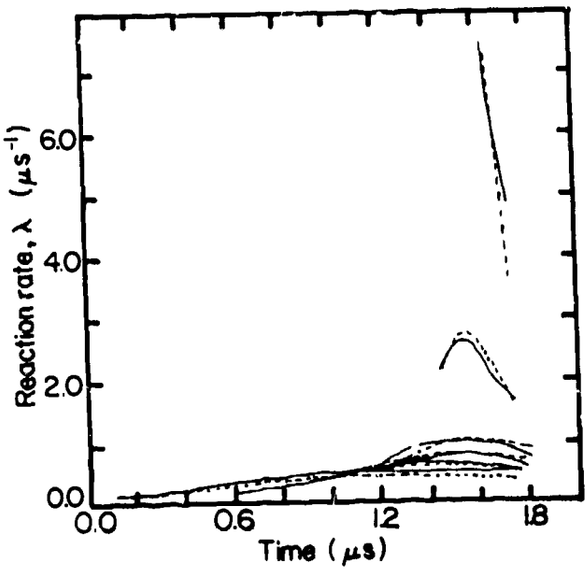

Fig. 5. Calculated reaction-rate histories at gauge locations.

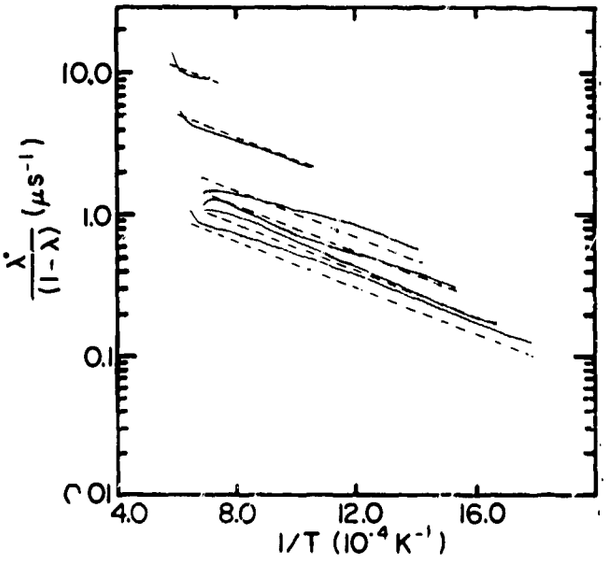

Fig. 6. Arrhenius representation of calculated reaction rates.

COMPUTER SIMULATIONS

A principal motive for determining empirical rate forms is to provide information for the modeling of initiation and detonation phenomena with numerical hydrodynamic calculations.[15] The successful simulations of experiments involving shock configurations and state conditions quite different from those used in obtaining the correlation allow more confidence in the generality of the derived rate. Such modeling is done with numerical hydrocodes that operate on the fluid dynamic conservation relations in finite difference form, advancing the calculation in small time increments, in the same sequence and somewhat the same manner as our direct analysis. However, instead of evaluating λ from the equation of state, an assumed rate law is used to update the reaction coordinate, and the $p(v,e,\lambda)$ relation is used to calculate the pressure for the next time cycle. In our simulations, we use the PAD 1D hydrocode developed by Fickett[15] with our addition of the HOM equation of state.

A first requirement of our rate law is that it gives simulations of the pressure data used to generate it. PAD calculations of the gauge-pressure histories are shown as dashed lines in Fig. 2. The good agreement signifies only that we made no serious

A more demanding test is simulation of gauge data with short-shock inputs. For TATB, we performed the same experiments described previously, except that the thick flyer (Fig. 1) was replaced with one that was 1 mm thick. A series of experiments gave the gauge records shown as solid lines in Fig. 7. Computer simulations with the calibrated DAGMAR form gave the dashed curves, in reasonably good agreement with observation. The calculated pressure-specific volume path at the impact face for these experiments is shown as the dotted curve in Fig. 5, and is seen to lie well below the region of calibration.

Another test of the rate is afforded by data from explosive wedge experiments. In this most common initiation experiment,[17] a planar shock is introduced into a wedge-shaped specimen, and the shock front progress is monitored with a streak camera as it builds up to detonation. The data are commonly displayed in "Pop-plot" form, relating the distance to detonation D to input shock pressure p_i as $D = Ap_i^{-B}$, with A and B constants. Our experiments on 1.8-g/cm^3 TATB were done with high-explosive driving systems, with shock strengths substantially higher and run distances much shorter than those of the embedded-gauge experiments. The streak-camera records typically displayed an initial constant wave velocity region, a break to an intermediate accelerating region, and a second break continuing to the onset of detonation. Both breaks fit the Pop-plot form, as shown by the open symbols in Fig. 8. Numerical hydrodynamic calculations of these buildup features, shown as crosses in Fig. 8, are in excellent agreement with observation.

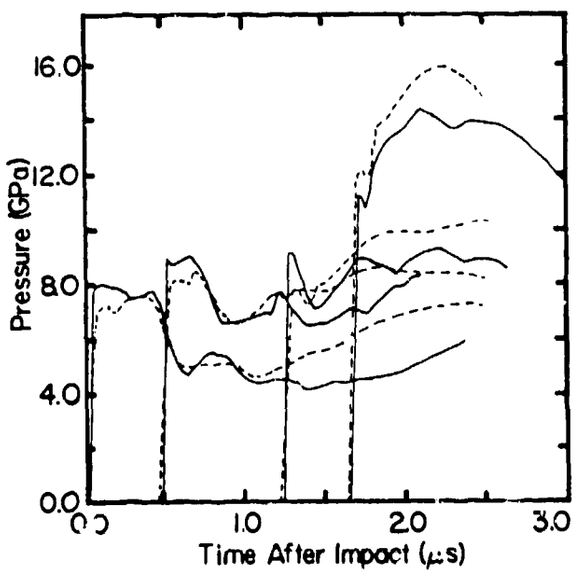

Fig. 7. Observed and calculated pressure histories with a short-shock input.

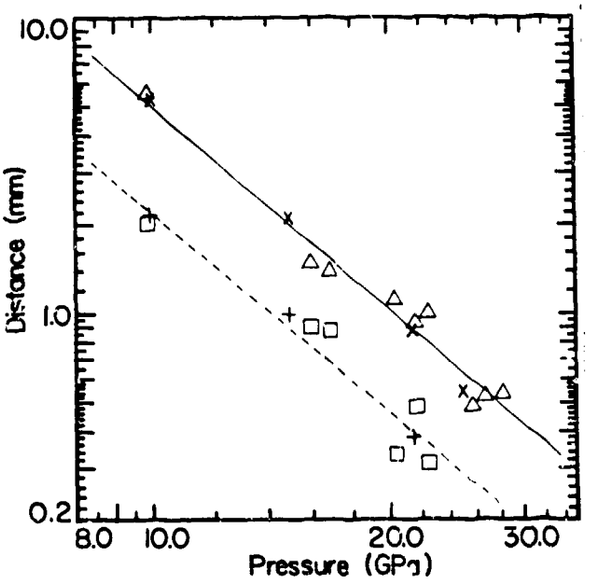

Fig. 8. Pop-plot representation of explosive-wedge data.

As discussed in Refs. 8 and 9, DAGMAR forms have provided computer simulations of nearly all of the existing planar shock initiation data base on PBX 9404 and 1.8-g/cm^3 TATB. The data base for PBX 9404 is substantial, including all of the experiments described above and numerous short-shock sensitivity tests and experiments in which plates are accelerated by partially reacted explosive. There are also high-pressure short-shock sensitivity test results for TATB, which we have also calculated successfully.

Thus far, we have found one experiment on TATB that we are unable to simulate. This is the reflected-pulse test shown in

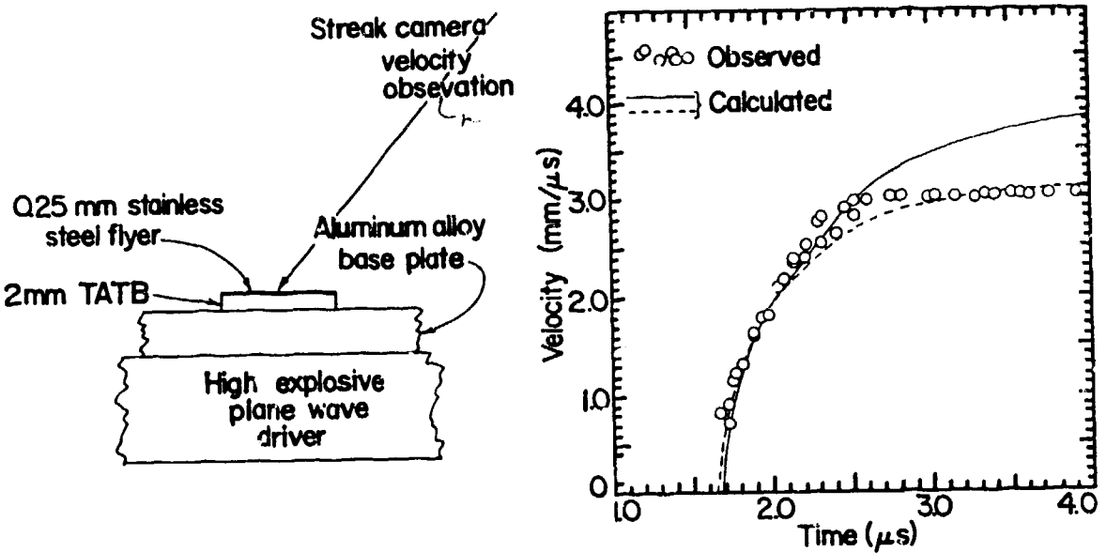

Fig. 9. Arrangement for reflected-pulse experiment and observed and calculated flyer velocity histories.

explosive slab, with a slab thickness that is less than the distance to detonation, and a mechanically high-impedance flyer reflects a short pressure pulse back into the reacting explosive. Observation of the plate acceleration with a streak camera provides a measure of the course of the decomposition when the pressure is nearly doubled and then reduced to zero. With DAGMAR, the effect is slight and involves only the temperature change, which is more affected by the ongoing reaction than by the pressure changes. Similar tests on PBX 9404 gave good agreement between computer simulation and experiment.[18] However, for TATB we observe plate terminal velocities that are significantly lower than we calculate with our calibrated rate (solid curve, see Fig. 9). The observed velocity history indicates a quenching of the rate when the rarefaction is reflected into the reacting explosive. We can model the plate velocity reasonably well, by arbitrarily stopping decomposition whenever the pressure in the flow falls below 5 GPa, as shown by the dashed curve. Although this artifice does not violate the derived rate form, which was calibrated to data all of which were above 7 GPa, it is an assumption that fails badly in computer simulations of the short-shock gauge data shown in Fig. 7.

DISCUSSION

It is well accepted that the shock-induced decomposition of heterogeneous explosives is effected by the formation of local high temperature regions, or hotspots, which are sites for subsequent burning processes or thermal explosions.[15,19] This notion of "nucleation and growth" of reaction is over three decades old,[20] and is quite consistent with empirical rate forms like DAGMAR that combine, multiplicatively, three factors in the rate, depending on shock strength, depletion and the current state of the material. Note that, in the only other complete exercise of our analysis procedure, Kanel and Dremin found that this combination best formulated a decomposition rate for TNT.[3,4]

These Soviet researchers, and others devising rate models,[15,21,22] have used a combination of the reaction progress variable and pressure for the current-state factor in the rate. The rationale for this lies in the almost universal observation that the linear burning rate of reactive solids is proportional to p^n.

phenomena we study, we note that, as combustion theory is more deeply developed, burning rates basically depend on an Arrhenius term in the solid-product interface temperature.[23] In addition, rate forms modified by current pressure generally do poorly in simulations of short-shock initiation data, as discussed in some detail in Refs. 10, 11, and 18.

With a rate depending on temperature in a manner universal to chemical kinetics, we are tempted to ascribe physical significance to a purely empirical construct. The temptation grows when we note a pair of modifications that can be made to DAGMAR. Inspection of Fig. 5 reveals that the right-hand end of the curves, representing the shock temperature, T_s, also lie along a straight line. The data thus admit to fitting by

$$\dot{\lambda}/(1-\lambda) = Z_1 \, e^{-T_1^*/T_s} \, e^{-T_2^*/T} \quad .$$

With $Z_1 = 262$, $T_1^* = 2378$, and $T_2^* = 1914$, we obtain correlations to the rates entirely as good as those shown in Figs. 4 or 5.* We also find that we have some flexibility in the choice of depletion factor. In particular, the correlation is as good with a factor $(1-\lambda)^{2/3}$, appropriate for three-dimensional phase-boundary controlled reaction,[24] as it is with simple depletion.

A serious obstacle remains to further interpretation of our empirical result in terms of thermal processes and chemical kinetics. This obstacle is, of course, our assumption of an equation of state that is based on temperature equilibrium for reacting, heterogeneous explosives. For these explosives, widely varied temperatures and hotspots are recognized as being necessary for the shock-induced decomposition to proceed at all. Although the strong correlation of our calculated temperature to an Arrhenius rate form suggests it must have some significant relation to the distribution of temperatures present in reacting explosive, this relationship is not known.

With our present equation-of-state limitation, contrived arguments to connect our rate to thermal kinetics must be made. First, we must explain why the activation temperatures (that is, the activation energies divided by the Boltzmann constant) derived from our observations are an order of magnitude below those determined by thermal analysis at atmospheric pressure. One explanation could be that very different activation energies pertain in the state regime of our observations than pertain in the near-ambient regime. Such an argument could be made on the basis of different rate-limiting processes in the context of Eyring's "starvation kinetics."[25] Another approach could be the quantum-mechanical calculations of Bardo, who derives a decrease in activation energy with imposed pressure,[26] but not of the magnitude we need.

As alternatives to these notions, we could assume that the atmospheric-pressure activation energies are valid in our observation region and apply the same argument about our calculated temperature that is used for molecular velocities in the chemical kinetics of gases. This would suggest that our equilibrium temperature represents the median of some temperature distribution, and that the relationship of the high-temperature tail of this distribution to realistic activation energies completely determines the reaction rate. Our measurements are thus of effective activation temperatures, scaled to realistic values through some

---

*Note that these constants give a sub-millisecond reaction time for an infinitesimal shock at ambient conditions; we trust that nature will not impose this extrapolation without warning.

consistently varying distribution function. Such a model could explain our observations on TATB that was of finer particle size, but the same density as that used in the work described above. The same explosive wedge and gauge experiments on this material (but no complete analysis) show it to have a much lower shock-induced decomposition rate than that of the coarser explosive. The same equation of state would apply, but the lower rate could be explained by arguing that the temperature distribution is narrower in the finer particle, more homogeneous explosive.

We presently find that the results of the reflected-pulse experiment described above are impossible to reconcile within the equilibrium temperature framework. The HOM equation of state just does not allow sufficient modification of the temperature by a rarefaction into partially reacted explosive to quench the rate. However, in other experiments, such as embedded-gauge and sensitivity measurements with short shocks, it is the very ability of the HOM/DAGMAR representation to sustain the reaction rate under rarefaction that produces excellent agreement with observation.

It appears to us that contriving physically sensible paths around our equation-of-state obstacle will prove to be more trouble than removing it. In our future work, the assumption of temperature equilibrium will be replaced with one that is more realistic for heterogeneous explosives. We plan to develop an analysis in the framework of continuum mixture theory,[27] and treat the reacting explosive as several discrete constituents at different temperatures. These constituents will include the unreacted solid, the products, a void fraction and probably a portion of hot solid. The temperature of this last constituent, or temperatures at solid-product "interfaces", will be the major variable that we will attempt to correlate to the rate.

While some progress has been made in some elements of this approach,[19,28-30] comparison to experiment has been superficial and ambiguous. This is largely because continuum mixture theory proliferates constitutive and rate relations for processes such as void collapse and energy transfer between constituents, each with a set of arbitrary constants. Reducing the arbitrariness with our type of experiments and analyses is a complicated and difficult task, particularly because the Lagrange analysis provides constitutive and rate relations for but a single progress variable. Abandoning temperature equilibrium thus may be replacing one very bad assumption with numerous questionable or arbitrary ones, and reaction rates in familiar chemical-kinetic forms may or may not survive the process. If they do, we may find our zealously sought connection between the fluid-dynamic and thermal analysis of the chemical kinetics of explosives decomposition.

REFERENCES

1. Some progress is being made with dynamic temperature measurements. See, for example D. D. Bloomquist and S. A. Sheffield in *Seventh Symposium (International) on Detonation*, Annapolis (June 1981) Preprints, p. 829.

2. M. Cowperthwaite in *Fourteenth Symposium (International) on Combustion* (The Combustion Institute, Pittsburg, 1973), p. 1259.

3. G. I. Kanel and A. N. Dremin, Fizika Goreniya i Vzryva 13, 85 (1977) English translation in Combustion, Explosion and Shock Waves 13, 71 (1977).

4. G. I. Kanel Fizika Goreniya i Vzryva 14, 113 (1978) English

5. M. Cowperthwaite and J. T. Rosenberg in *Sixth Symposium (International) on Detonation*, Office of Naval Research report ACR-221 (1976) p. 786.

6. M. Cowperthwaite, ibid. Ref. 1, p. 256.

7. H. C. Vantine, et. al, ibid. Ref. 1, p. 593.

8. M. Cowperthwaite and J. T. Rosenberg, ibid, Ref. 1, p. 835.

9. Jerry Wackerle, J. O. Johnson, and P. M. Halleck, ibid. Ref. 5, p. 20.

10. Jerry Wackerle, R. L. Rabie, M. J. Ginsberg, and A. B. Anderson in *Behaviour of Dense Media Under High Dynamic Pressures, Symposium H.D.P.*, Paris (1978), p. 127.

11. Allan B. Anderson, M. J. Ginsberg, W. L. Seitz, and Jerry Wackerle, ibid. Ref. 1, p. 584.

12. Harry Vantine, et. al, Rev. Sci. Instrum. 51, 116 (1980).

13. H. C. Vantine, L. M. Erickson, and J. A. Janzen, J. Appl. Phys. 3, 1957 (1980).

14. Lynn Seaman, J. Appl. Phys. 45, 1303 (1974).

15. Charles L. Mader, *Numerical Modeling of Detonation*, (University of California Press, Berkley, 1979).

16. Charles L. Mader and C. A. Forest, Los Alamos report LA-6259 (1976).

17. J. B. Ramsay and A. Popolato in *Fourth Symposium (International) on Detonation*, Office of Naval Research report ACR-126 (1965), p. 233.

18. Jerry Wackerle and A. B. Anderson, Bull. APS Series II, 24, 718 (1978).

19. A. W. Campbell, W. C. Davis, J. B. Ramsay, and J. R. Travis, Phys. Fluids 4, 511.

20. Henry Eyring, Richard E. Powell, George H. Duffey, and Ramson B. Parlin, Chem. Rev. 45, 69 (1949).

21. B. D. Trott and R. G. Jung in *Fifth Symposium (International) on Detonation*, Office of Naval Research report ACR-184 (1970), p. 191.

22. E. L. Lee and C. M. Tarver, Phys. Fluids 23, 2362 (1980).

23. Forman H. Williams, *Combustion Theory* (Addison-Wesley, Palo Alto, 1965) Chapter 9.

24. Tong B. Tang and M. M. Chaudhri, J. Thermal Analysis 17, p. 359 (1979).

25. Henry Eyring, Science 199, 740 (1978).

26. Richard D. Bardo, ibid. Ref. 1, p. 74.

27. Ray M. Bowen in *Continuum Physics*, Vol. III (Academic Press, New York, 1976) Part I.

28. A. A. Shilperoord, ibid. Ref. 5, p. 371.

29. J. W. Nunziato, E. K. Walsh, and J. E. Kennedy, ibid. Ref. 10, p. 139.

30. Y. Partom, ibid. Ref. 1, p. 262.